HHS Public Access

Author manuscript

Free Radic Biol Med. Author manuscript; available in PMC 2020 November 17.

Published in final edited form as:

Free Radic Biol Med. 2014 August ; 73: 291–298. doi:10.1016/j.freeradbiomed.2014.05.019.

Suberoylanilide hydroxamic acid radiosensitizes tumor hypoxic cells in vitro through the oxidation of nitroxyl to nitric oxide

Yuval Samuni[a,b], **David A. Wink**[c], **Murali C. Krishna**[c], **James B. Mitchell**[c], **Sara Goldstein**[d,*]

[a]IMPACT Strategic Research Centre, Deakin University School of Medicine, Geelong, VIC 3220, Australia

[b]Department of Oral and Maxillofacial Surgery, Barzilai Medical Center, Ashkelon 78278, Israel

[c]Radiation Biology Branch, National Cancer Institute, National Institutes of Health, Bethesda, MD 20892, USA

[d]Institute of Chemistry, The Accelerator Laboratory, The Hebrew University of Jerusalem, Jerusalem 91904, Israel

Abstract

The pharmacological effects of hydroxamic acids are partially attributed to their ability to serve as HNO and/or NO donors under oxidative stress. Previously, it was concluded that oxidation of the histone deacetylase inhibitor suberoylanilide hydroxamic acid (SAHA) by the metmyoglobin/H_2O_2 reaction system releases NO, which was based on spin trapping of NO and accumulation of nitrite. Reinvestigation of this system demonstrates the accumulation of N_2O, which is a marker of HNO formation, at similar rates under normoxia and anoxia. In addition, the yields of nitrite that accumulated in the absence and the presence of O_2 did not differ, implying that the source of nitrite is other than autoxidation of NO. In this system metmyoglobin is instantaneously and continuously converted into compound II, leading to one-electron oxidation of SAHA to its respective transient nitroxide radical. Studies using pulse radiolysis show that one-electron oxidation of SAHA (pK_a=9.56 ± 0.04) yields the respective nitroxide radical (pK_a=9.1 ± 0.2), which under all experimental conditions decomposes bimolecularly to yield HNO. The proposed mechanism suggests that compound I oxidizes SAHA to the respective nitroxide radical, which decomposes bimolecularly in competition with its oxidation by compound II to form HNO. Compound II also oxidizes HNO to NO and NO to nitrite. Given that NO, but not HNO, is an efficient hypoxic cell radiosensitizer, we hypothesized that under an oxidizing environment SAHA might act as a NO donor and radiosensitize hypoxic cells. Preincubation of A549 and HT29 cells with 2.5 μM SAHA for 24 h resulted in a sensitizer enhancement ratio at 0.01 survival levels ($SER_{0.01}$) of 1.33 and 1.59, respectively. Preincubation of A549 cells with oxidized SAHA had hardly any effect and, with 2 mM valproic acid, which lacks the hydroxamate group, resulted in $SER_{0.01}$=1.17. Preincubation of HT29 cells with SAHA and Tempol, which readily oxidizes HNO to NO, enhanced the radiosensitizing effect of SAHA. Pretreatment with SAHA blocked A549

*Corresponding author. Fax: +972 2 6586416. sara.goldstein1@mail.huji.ac.il (S. Goldstein).

Appendix A. Supplementary Information

Supplementary data associated with this article can be found in the online version at http://dx.doi.org/10.1016/j.freeradbiomed.2014.05.019.

cells at the G1 stage of the cell cycle and upregulated γ-H2AX after irradiation. Overall, we conclude that SAHA enhances tumor radioresponse by multiple mechanisms that might also involve its ability to serve as a NO donor under oxidizing environments.

Keywords

SAHA; Valproic acid; Tempol; Pulse radiolysis; HNO; NO; Nitroxide; Kinetics; Free radicals

Suberoylanilide hydroxamic acid (SAHA; Fig. 1), an inhibitor of histone deacetylase (HDAC), is known to cause cell growth arrest and apoptosis [1]. Clinical evaluation of the drug is currently under way in multiple studies of patients with hematologic and solid tumor malignancies [2–4].

Part of the biological activities of hydroxamic acids is linked to their capacity to generate nitric oxide (NO) and/or its reduced form HNO/NO^- (nitroxyl) [5–10]. The latter is an unstable weak acid (pK_a = 11.4 [11,12]), which readily decomposes to yield N_2O [12], and like NO displays both pro-oxidative and antioxidative effects [13–16]. It has been reported that oxidation of SAHA by the metmyoglobin/H_2O_2 reaction system releases NO based on spin trapping of NO by carboxy-PTIO and accumulation of nitrite, assuming that it is formed via NO reaction with O_2 [9]. However, carboxy-PTIO cannot be used to distinguish NO from HNO because it reacts with both and oxidizes HNO to NO [17], and the source of nitrite might be other than autoxidation of NO. Recently, it was demonstrated that oxidation of acetohydroxamic and glycine-hydroxamic acids by the metmyoglobin/H_2O_2 reaction system generates HNO and nitrite under both anoxia and normoxia [18]. In line with these results we reinvestigated the oxidation of SAHA by this system and extended this study to oxidation of SAHA by radiolytically borne radicals demonstrating that HNO is the precursor of NO.

Even though HDAC inhibitors have shown promise as candidate radiosensitizers for many types of cancers [19–22], their mechanisms of actions are not well understood. Given that NO, but not HNO, radiosensitizes hypoxic cells in vitro [23–28], we hypothesized that a plausible mechanism by which SAHA enhances tumor radioresponse involves its ability to serve as a NO donor under oxidizing environments thus adding an advantage over other HDAC inhibitors lacking the hydroxamate group. This study demonstrates that one-electron oxidation of SAHA forms HNO, which is partially oxidized to NO under an oxidizing environment. It is also demonstrated that SAHA is a more efficient radiosensitizer of hypoxic tumor cells compared to oxidized SAHA or valproic acid lacking the hydroxamate moiety.

Material and methods

Materials

Water for solution preparation was purified using a Milli-Q system. SAHA was received from Merck & Co. (Whitehouse Station, NJ, USA) and from LC Laboratories. Valproic acid, Tempol, and myoglobin from horse heart were purchased from Sigma (St. Louis, MO, USA). Diethylenetriamine nonoate (DETA/NO) was purchased from Cayman Chemical

(Ann Arbor, MI, USA). Sephadex G-25 for gel-filtration chromatography was purchased from Pharmacia (Uppsala, Sweden). Metmyoglobin ($MbFe^{III}$) was prepared by adding excess of ferricyanide to myoglobin in 5–50 mM phosphate buffer at pH 7 followed by chromatographic separation through a Sephadex G-25 column. Ferryl myoglobin ($MbFe^{IV}=O$) was prepared by mixing $MbFe^{III}$ with excess of H_2O_2 followed by addition of catalase to remove residual unreacted H_2O_2. The concentrations of $MbFe^{III}$ and $MbFe^{IV}=O$ were determined spectrophotometrically using $\varepsilon_{408}=188\ mM^{-1}\ cm^{-1}$ and $\varepsilon_{421}=111\ mM^{-1}\ cm^{-1}$, respectively [29]. Oxidized SAHA was prepared via its reaction with $MbFe^{IV}=O$ followed by the removal of the protein using Sephadex G-25 column chromatography. Griess reagents were prepared according to a previously published method [30]. Stock solutions of SAHA were prepared in dimethyl sulfoxide (DMSO) and that of DETA/NO in 0.01 M NaOH.

Nitrite analysis

Nitrite was assayed by mixing equal volumes of the sample and the Griess reagent. Analysis of nitrite produced under anoxia was done through the injection of 1 ml anoxic sample into 1 ml anoxic reagent, which was placed in a cell sealed with a rubber septum. The absorption at 540 nm was read 15 min after the addition of the sample. Calibration curves were prepared using known concentrations of nitrite.

Gas chromatography (GC)

Sample solutions (5 ml) were placed in a glass vial (10.7 ml) sealed with a rubber septum. An aliquot of the reaction headspace (2 ml) was taken and 1 ml at room pressure and temperature was injected onto a 5890 Hewlett–Packard gas chromatograph equipped with a thermal conductivity detector, a 10-ft-⅛-in. Porapak Q column at an operating oven temperature of 70 °C (injector and detector 150 °C) and a flow rate of 20 ml/min (He, carrier gas). The retention times of O_2/N_2 and N_2O were 0.8 and 2.8 min, respectively. The yields of N_2O were calculated on the basis of a standard curve prepared by injecting known amounts of N_2O gas (Maxima, Israel).

Irradiation

Pulse radiolysis experiments were carried out using a 5-MeV Varian 7715 linear accelerator (0.1- to 1.5-μs electron pulses, 200-mA current). A 200-W Xe lamp produced the analyzing light. Appropriate cutoff filters were used to minimize photochemistry. Measurements were done using a 2-cm Spectrosil cell with three light passes. All experiments were done at room temperature.

Steady-state irradiations were carried out at room temperature using either a Precision X-Ray X-Rad 320 (East Haven, CT, USA) operating at 300 kV/10 mA with a 2-mm aluminum filter (2.42 Gy min^{-1}) or a ^{137}Cs source (6.4 Gy min^{-1}). The dose rate at 50 cm from the X-ray source was determined by multiple thermoluminescence dosimeter readings and that of the ^{137}Cs source using the Fricke dosimeter.

Cell culture

Human A549 lung adenocarcinoma and HT29 colon adenocarcinoma cells were cultured at 37 °C in RPMI medium supplemented with 10% (v/v) fetal calf serum, 100 U/ml penicillin, and 100 U/ml streptomycin, in a 95% air/5% CO_2 incubator. Stock cultures of exponentially growing cells were trypsinized, rinsed, plated (3×10^5 cells per glass flask) in 25-cm^2 glass flasks, and incubated for 16 h at 37 °C before experimental protocols. Cells were exposed to 2.5 μM SAHA for 24 h and then subjected to hypoxia (detailed below) for 1 h and irradiated.

Induction of hypoxia

Cells from stock cultures were trypsinized, plated into 25-cm^2 glass flasks (3×10^5 cells/flask), and incubated 16 h before each experiment. Flasks were sealed with soft rubber stoppers, and 19-gauge needles were pushed through to act as entrance and exit ports for the humidified gas mixture. Stoppered flasks connected in series and mounted on a reciprocating platform (agitated at 1 Hz) were gassed at 37 °C for 1 h with 5% CO_2/95% N_2. The gassing procedure resulted in an equilibrium between the gas and the liquid phase and yielded oxygen concentrations in the effluent gas phase of < 10 ppm as measured by a Thermox probe [31].

Clonogenic assay

Cells were trypsinized, diluted, and plated in triplicates for macroscopic colony formation. Plates were incubated for 10–12 days, after which colonies were fixed with methanol/acetic acid, 3/1 (v/v), stained with crystal violet, and counted. Colonies containing > 50 cells were scored.

Flow cytometry and cell cycle phase analysis

After treatment A549 cells were rinsed with phosphate-buffered saline (PBS), trypsinized, fixed with 70% ethanol, incubated with 50 mg/ml propidium iodide, and analyzed for DNA content by using a BD FACSscan (BD Biosciences, San Jose, CA, USA).

Immunoblot analysis for γ-H2AX

After treatment A549 cells were harvested and lysed in 10 mM Hepes, pH 7.9,1.5 mM $MgCl_2$,10 mM KCl with 0.5 mM dithiothreitol and 1.5 mM phenylmethanesulfonyl fluoride with complete protease inhibitor cocktail (Roche Applied Science, Indianapolis, IN, USA). Histones from the nuclear pellet were extracted in 0.2 M sulfuric acid by incubating samples on ice for 4–6 h. After centrifugation, acid-soluble histones were transferred to fresh tubes and 9 volumes of ice-cold acetone were added. Histones were precipitated at −20 °C overnight and were pelleted by centrifugation at 14,000 rpm for 10 min at 4 °C. Supernatant was discarded and pellets were air-dried. Histones were solubilized in 4 M urea and protein concentration was determined by Bio-Rad D_c protein assay. Histones were separated on 4–10% Tris-glycine gels (Invitrogen, Carlsbad, CA, USA) by loading 20 μg samples and transferred to nitrocellulose membrane using the iBlot dry blotting system from Invitrogen. Membranes were incubated overnight at 4 °C with mouse monoclonal anti-phospho-histone H2AX (Ser139), clone JBW301 (1:10,000) from Millipore (Temecula, CA, USA), washed three times with PBS-Tween 20 and incubated with horseradish peroxidase-conjugated anti-

mouse antibody (Santa Cruz Biotechnology, Santa Cruz, CA, USA). γ-H2AX was visualized using an ECL detection kit (PerkinElmer, Waltham, MA, USA) using a Fluor Chem SP imager (Alpha Innotech, San Leandro, CA, USA). Membranes were stripped using Re-Blot Plus mild antibody stripping solution (Millipore) and reprobed with 1:1000 rabbit antiserum to histone H2A (acidic patch from Millipore) to ascertain uniform loading. Signal intensities were normalized to their loading control H2A and expressed as fold change compared to controls.

Results and discussion

Oxidation of SAHA by radiolytically borne radicals

SAHA contains an aromatic group (Fig. 1), and therefore the oxidation of its hydroxamate moiety was achieved and studied using $Br_2^{\bullet -}$ and $^{\bullet}N_3$ radicals, which react extremely slowly, if at all, with aromatic groups, and with DMSO used to solubilize SAHA. When N_2O-saturated solutions (pH > 3) are irradiated, $^{\bullet}OH$ is produced via reactions (1) and (2):

$$H_2O \rightarrow e_{aq}^{-}(2.6),\ {}^{\bullet}OH\ (2.7),\ H^{\bullet}\ (0.6),\ H_3O^{+}\ (2.6),\ H_2O_2\ (0.72) \quad (1)$$

The numbers in parentheses are G values, which represent their respective yields (in 10^{-7} M Gy^{-1}), which are about 7% higher in the presence of high solute concentrations.

$$e_{aq}^{-} + N_2O + H_2O \rightarrow {}^{\bullet}OH + N_2 + OH^{-};\ k_2 = 9.7 \times 10^9\ M^{-1}\ s^{-1}\ [32] \quad (2)$$

The oxidation of bromide or azide ions by $^{\bullet}OH$ generates $Br_2^{\bullet -}$ and $^{\bullet}N_3$ radicals, respectively. Because stock solutions of SAHA were prepared as 0.25 M in DMSO ([DMSO]/[SAHA] ≈ 56), the concentrations of bromide or azide ions were sufficiently high to compete efficiently with DMSO for $^{\bullet}OH$.

The second-order decay of 1 μM $Br_2^{\bullet -}$ followed at 360 nm (ε=9500 $M^{-1}cm^{-1}$) turned into first-order decay in the presence of [SAHA] > 50 μM. The bimolecular rate constant was determined from the dependence of the observed first-order rate constant on [SAHA] (e.g., Supplementary Fig. 1S), which decreased as the pH decreased (Fig. 2), implying that the oxidation of the deprotonated form of SAHA is more efficient than that of the protonated one, i.e., $(4.9 \pm 0.1) \times 10^7$ and $(3.0 \pm 0.7) \times 10^6$ $M^{-1}s^{-1}$, respectively. The dependence of the rate constant on the pH allows the determination of the pK_a=9.56 ± 0.04 for SAHA in aqueous solutions, which is significantly lower than that determined in 70%/30% (v/v) water/DMSO, i.e., 11.65 [33].

The rate constant of $^{\bullet}N_3$ reaction with the deprotonated form of SAHA has been determined to be $(5.1 \pm 0.1) \times 10^9$ M^{-1} s^{-1} using competition kinetics against phenol at pH 12 by following the formation of $C_6H_5O^{\bullet}$ at 400 nm (Supplementary Fig. 2S). The reactions of $^{\bullet}N_3$ with 0.12–1 mM SAHA was studied directly by following the formation and decomposition of the transient nitroxide radical at λ 280–340 nm (Fig. 3).

The dependence of the absorption on the pH (Fig. 3, inset) allows the determination of pK_a=9.1 ± 0.2 for RC(O)NHO$^{\bullet}$, which is similar to that previously determined for CH3C(O)NHO$^{\bullet}$ [10].

Under all experimental conditions the decay of the nitroxide radical obeyed second-order kinetics. The bimolecular rate constant of the deprotonated form has been determined to be $2k$= (8.9 ± 0.8) × 10^7 M^{-1} s^{-1} at ionic strength I = 0.2 M. This process leads to the formation of an intermediate, which decomposes via a first-order reaction into another transient species having a maximum absorption at 310 nm (Fig. 4B). The rate constant of this reaction was determined to be 50 ± 4 s^{-1} at pH 11.4 by following the formation of the absorption of this intermediate at λ > 330 nm at which the contribution of the second-order decay is negligible. This transient species decayed via a first-order reaction and its rate constant increased as [OH^-] or [SAHA] increased, resulting in k=3.2 × 10^3 × [SAHA] + 57 × [OH^-] s^{-1}. Typical kinetic traces at 285 and 312 nm are given in Fig. 4A and B, respectively.

Similar results have been reported for the decomposition of $CH_3C(O)NO^{\bullet-}$ for which it has been proposed that the bimolecular process forms several adducts due to the distribution of the spin over the O–C–N–O group [10]. Some of the adducts decompose, yielding unidentified products; others decompose to yield RC(O) N = O, which decomposes via hydrolysis (catalyzed by OH^-) or via the reaction with $RC(O)NHO^-$ forming HNO (Scheme 1).

The accumulation of nitrite was assayed by the Griess reagent only in the bromide system owing to quenching of the dye by azide ions. Steady-state irradiation (128–267 Gy) of N_2O-saturated solutions containing 0.4 mM SAHA and 0.3 M NaBr at pH 10.4 hardly yielded nitrite after the mixing of the irradiated sample with aerated reagent.

Because N_2O accumulation cannot be monitored by GC in N_2O-saturated solutions ([N_2O] 24 mM), the solutions were deoxygenated with He and H_2O_2 was used instead of N_2O to convert e^-_{aq} into $^{\bullet}OH$ [32]. Pulse or γ-irradiation of anoxic solutions containing 0.5 mM SAHA, 0.5 mM H_2O_2, and 0.4 M NaN_3 at pH 10 generated N_2O resulting in [HNO]/[$^{\bullet}N_3$] = 0.08 ± 0.02, i.e., the bimolecular decomposition of the transient nitroxide radical yields about 16% HNO.

Oxidation of SAHA by the $MbFe^{III}/H_2O_2$ reaction system

The reaction between $MbFe^{III}$ and H_2O_2 produces a two-electron oxidizing intermediate ($^{\bullet}MbFe^{IV}$=O, compound I) and a relatively more stable one-electron oxidizing product ($MbFe^{IV}$=O, compound II). $MbFe^{III}$ does not react with SAHA, but upon the addition of H_2O_2 it is converted within less than 30 s into $MbFe^{IV}$=O. $MbFe^{III}$ is recycled, but its steady-state concentration is hardly detectable as evident from the absence of its characteristic absorbance at 408 nm (Supplementary Fig. 3S). The absorption of $MbFe^{IV}$=O progressively decayed at both 422 and 500–650 nm without any appearance of $MbFe^{III}$ (Supplementary Fig. 3S), which most probably reflects deterioration of the heme owing to iron release [34].

The rate of nitrite accumulation decreased with time owing to the irreversible destruction of the heme. Therefore, we compared only the initial rates of nitrite release, which increased upon increasing [$MbFe^{III}$], but were hardly affected by varying [SAHA] between 0.25 and 4 mM or [H_2O_2] between 0.5 and 5 mM as previously reported [9]. However, the accumulation of nitrite under anoxic conditions was similar to that under normoxia (Fig. 5), implying that the source of nitrite is other than autoxidation of NO.

Analysis by GC of the headspace of anoxic or aerated solutions containing 30 μM $MbFe^{III}$, 5 mM H_2O_2, and 2 mM SAHA demonstrated that accumulation of N_2O under anoxia is similar to that under normoxia (Fig. 6).

Under the same experimental conditions the rate of nitrite accumulation exceeded that of N_2O, e.g., in the presence of 10 μM $MbFe^{III}$, 5 mM H_2O_2, and 2 mM SAHA the rates of N_2O and nitrite accumulation were 0.42 ± 0.05 and 5.6 ± 0.2 μM/min, respectively.

Similar results have been reported for acetohydroxamic and glycine-hydroxamic acids [18]. It is suggested that compound I oxidizes the hydroxamate to its respective nitroxide radical, which decomposes bimolecularly in competition with its oxidation by compound II yielding HNO. This decomposes to N_2O in competition with its oxidation by compound II to NO, which is further oxidized more efficiently by compound II to nitrite (Scheme 2).

SAHA enhances the killing of irradiated hypoxic cells

The experimental setup included preincubation of the cells with 2.5 μM SAHA under aerobic conditions followed by 1 h hypoxia under which radiation was performed. The cells were preincubated for 24 h with SAHA because preincubation for 1 h had a small effect on the cell survival. The survival curves of the irradiated cells were corrected for SAHA cytotoxicity. The sensitizer enhancement ratio was determined at the 0.01 survival level ($SER_{0.01}$; the ratio of radiation doses for hypoxia control and hypoxia plus SAHA) to be 1.33 for A549 cells (Fig. 7) and 1.59 for HT29 cells (Fig. 8).

The NO donor DETA/NO, which decomposes to yield two molecules of NO with $t_{1/2}$=20 h at 37 °C [35], radiosensitized hypoxic A549 cells under the same experimental conditions used for SAHA (Fig. 9), suggesting that the effect of SAHA might be due to the formation of NO.

To better understand the role of the hydroxamate moiety of SAHA, we repeated the experiment with oxidized SAHA. The results presented in Fig. 10 demonstrate that oxidized SAHA is not a radiosensitizer of hypoxic cells. The minor effect of the oxidized drug could result from incomplete oxidation of the drug.

The effect of valproic acid (Fig. 1), which is an HDAC inhibitor lacking the hydroxamate moiety, on the killing of irradiated hypoxic A549 cells was observed at relatively high concentrations of 2 mM at which $SER_{0.01}$ = 1.17 (Fig. 11).

Such high concentrations of valproic acid (millimolar range) were required to radiosensitize other aerobic cancer cell lines [36–39], indicating that SAHA is a more efficient radiosensitizer.

The results presented in Figs. 10 and 11 demonstrate the importance of the hydroxamate moiety. If one-electron oxidation of the hydroxamate forms HNO initially, the addition of Tempol might increase the radiation sensitivity because Tempol readily oxidizes HNO to NO [40]. Indeed, preincubation of HT29 cells with 2.5 μM SAHA and 1 mM Tempol enhanced the radiation sensitivity of SAHA as demonstrated in Fig. 12.

Previously, it has been reported that preincubation for 18 h with 1–2 μM SAHA under hypoxia (1% O_2) enhanced the radiation (5 Gy)-induced killing of carcinoma cell lines, including HT29 cells [41]. Interestingly, our results show that higher radiation doses were required for radiosensitization by SAHA. This differential in radioresistance of cancer cells might result from the difference in O_2 concentration because in our experiments the concentration of O_2 in the gas phase is less than 0.001%, i.e., practically anoxic conditions.

Preincubation of the cells for 24 h with 2.5 μM SAHA under aerobic conditions blocked them at the G1 cell cycle stage (Fig. 13), implying that SAHA treatment is associated with redistribution of cell populations into radiosensitive cell cycle phases.

Immunoblot analysis of phosphorylated histone H2AX (γ-H2AX) was used as an indicator of DNA damage [42]. As shown in Fig. 14, γ-H2AX induction is evident a few hours postirradiation (8 Gy) of hypoxic A549 cells. These results are similar to those reported for the combination of radiation and SAHA, NO, or NO donors under normoxia or hypoxia [20,27,43].

In conclusion, our results demonstrate that one-electron oxidation of SAHA generates HNO, oxidized SAHA has hardly any effect, and SAHA is a more efficient radiosensitizer than valproic acid. Given that HNO, but not NO, failed to radiosensitize hypoxic cells and that Tempol enhanced the radiation sensitivity of SAHA, we conclude that one of the mechanisms by which SAHA enhances tumor radioresponse might involve its ability to form NO under oxidizing environments.

Supplementary Material

Refer to Web version on PubMed Central for supplementary material.

Acknowledgment

This work has been supported by the Israel Science Foundation.

References

[1]. Butler LM; Agus DB; Scher HI; Higgins B; Rose A; Cordon-Cardo C; Thaler HT; Rifkind RA; Marks PA; Richon VM Suberoylanilide hydroxamic acid, an inhibitor of histone deacetylase, suppresses the growth of prostate cancer cells in vitro and in vivo. Cancer Res. 60:5165–5170; 2000. [PubMed: 11016644]

[2]. Siegel D; Hussein M; Belani C; Robert F; Galanis E; Richon VM; Garcia-Vargas J; Sanz-Rodriguez C; Rizvi S Vorinostat in solid and hematologic malignancies. J. Hematol. Oncol. 2:31; 2009. [PubMed: 19635146]

[3]. Vansteenkiste J; Van Cutsem E; Dumez H; Chen C; Ricker JL; Randolph SS; Schoffski P Early phase II trial of oral vorinostat in relapsed or refractory breast, colorectal, or non-small cell lung cancer. Invest. New Drugs 26:483–488; 2008. [PubMed: 18425418]

[4]. Gryder BE; Sodji QH; Oyelere AK Targeted cancer therapy: giving histone deacetylase inhibitors all they need to succeed. Future Med. Chem 4:505–524; 2012. [PubMed: 22416777]

[5]. Gladwin MT; Shelhamer JH; Ognibene FP; Pease-Fye ME; Nichols JS; Link B; Patel DB; Jankowski MA; Pannell LK; Schechter AN; Rodgers GP Nitric oxide donor properties of hydroxyurea in patients with sickle cell disease. Br. J. Haematol. 116:436–444; 2002. [PubMed: 11841449]

[6]. King SB The nitric oxide producing reactions of hydroxyurea. Curr. Med. Chem. 10:437–452; 2003. [PubMed: 12570692]

[7]. Marmion CJ; Griffith D; Nolan KB Hydroxamic acids–an intriguing family of enzyme inhibitors and biomedical ligands. Eur. J. Inorg. Chem. 2004:3003–3016; 2004.

[8]. Burkitt MJ; Raafat A Nitric oxide generation from hydroxyurea: significance and implications for leukemogenesis in the management of myeloproliferative disorders. Blood 107:2219–2222; 2006. [PubMed: 16282342]

[9]. Samuni Y; Flores-Santana W; Krishna MC; Mitchell JB; Wink DA The inhibitors of histone deacetylase suberoylanilide hydroxamate and trichostatin A release nitric oxide upon oxidation. Free Radic. Biol. Med. 47:419–423; 2009. [PubMed: 19447172]

[10]. Goldstein S; Samuni A One-electron oxidation of acetohydroxamic acid: the intermediacy of nitroxyl and peroxynitrite. J. Phys. Chem. A 115:3022–3028; 2011. [PubMed: 21425838]

[11]. Bartberger MD; Liu W; Ford E; Miranda KM; Switzer C; Fukuto JM; Farmer PJ; Wink DA; Houk KN The reduction potential of nitric oxide (NO) and its importance to NO biochemistry. Proc. Natl. Acad. Sci. USA 99:10958–10963; 2002. [PubMed: 12177417]

[12]. Shafirovich V; Lymar SV Nitroxyl and its anion in aqueous solutions: spin states, protic equilibria, and reactivities toward oxygen and nitric oxide. Proc. Natl. Acad. Sci. USA 99:7340–7345; 2002. [PubMed: 12032284]

[13]. Fukuto JM; Bartberger MD; Dutton AS; Paolocci N; Wink DA; Houk KN The physiological chemistry and biological activity of nitroxyl (HNO): the neglected, misunderstood, and enigmatic nitrogen oxide. Chem. Res. Toxicol. 18:790–801; 2005. [PubMed: 15892572]

[14]. Hewett SJ; Espey MG; Uliasz TF; Wink DA Neurotoxicity of nitroxyl: insights into HNO and NO biochemical imbalance. Free Radic. Biol. Med. 39:1478–1488; 2005. [PubMed: 16274883]

[15]. Lopez BE; Shinyashiki M; Han TH; Fukuto JM Antioxidant actions of nitroxyl (HNO). Free Radic. Biol. Med. 42:482–491; 2007. [PubMed: 17275680]

[16]. Switzer CH; Flores-Santana W; Mancardi D; Donzelli S; Basudhar D; Ridnour LA; Miranda KM; Fukuto JM; Paolocci N; Wink DA The emergence of nitroxyl (HNO) as a pharmacological agent. Biochim. Biophys. Acta 835–840:2009; 1787.

[17]. Samuni U; Samuni Y; Goldstein S On the distinction between nitroxyl and nitric oxide using nitronyl nitroxides. J. Am. Chem. Soc. 132:8428–8432; 2010. [PubMed: 20504018]

[18]. Samuni Y; Samuni U; Goldstein S The mechanism underlying nitroxyl and nitric oxide formation from hydroxamic acids. Biochim. Biophys. Acta 1820:1560–1566; 2012. [PubMed: 22634736]

[19]. Chinnaiyan P; Vallabhaneni G; Armstrong E; Huang SM; Harari PM Modulation of radiation response by histone deacetylase inhibition. Int. J. Radial Oncol. Biol. Phys. 62:223–229; 2005.

[20]. Munshi A; Tanaka T; Hobbs ML; Tucker SL; Richon VM; Meyn RE Vorinostat, a histone deacetylase inhibitor, enhances the response of human tumor cells to ionizing radiation through prolongation of gamma-H2AX foci. Mol. Cancer Ther 5:1967–1974; 2006. [PubMed: 16928817]

[21]. Camphausen K; Tofilon PJ Inhibition of histone deacetylation: a strategy for tumor radiosensitization. J. Clin. Oncol. 25:4051–4056; 2007. [PubMed: 17827453]

[22]. Groselj B; Sharma NL; Hamdy FC; Kerr M Kiltie, A. E. Histone deacetylase inhibitors as radiosensitisers: effects on DNA damage signalling and repair. Br. J. Cancer 108:748–754; 2013. [PubMed: 23361058]

[23]. Mitchell JB; Wink DA; Degraff W; Gamson J; Keefer LK; Krishna MC Hypoxic mammalian-cell radiosensitization by nitric-oxide. Cancer Res. 53:5845–5848; 1993. [PubMed: 8261391]

[24]. Mitchell JB; Cook JA; Krishna MC; DeGraff W; Gamson J; Fisher J; Christdodoulou D; Wink DA Radiation sensitisation by nitric oxide releasing agents. Br. J. Cancer 74:S181–S184; 1996.

[25]. Mitchell JB; DeGraff W; Kim S; Cook JA; Gamson J; Christodoulou D; Feelisch M; Wink DA Redox generation of nitric oxide to radiosensitize hypoxic cells. Int.J. Radial. Oncol. Biol. Phys. 42:795–798; 1998.

[26]. Policastro L; Duran H; Henry Y; Molinari B; Favaudon V Selective radio sensitization by nitric oxide in tumor cell lines. Cancer Lett. 248:123–130; 2007. [PubMed: 16899337]

[27]. Wardman P; Rothkamm K; Folkes LK; Woodcock M; Johnston PJ Radiosensitization by nitric oxide at low radiation doses. Radiat. Res 167:475–484; 2007. [PubMed: 17388699]

[28]. Folkes LK; O'Neill P Modification of DNA damage mechanisms by nitric oxide during ionizing radiation. Free Radic. Biol. Med. 58:14–25; 2013. [PubMed: 23376236]

[29]. Antonini E; Brunori M Hemoglobin and Myoglobin in Their Reactions with Ligands. Amsterdam: North-Holland; 1971.

[30]. Green LC; Wagner DA; Glogowski J; Skipper PL; Wishnok JS; Tannenbaum SR Analysis of nitrate, nitrite, and [^{15}N]nitrate in biological fluids. Anal. Biochem. 126:131–138; 1982. [PubMed: 7181105]

[31]. Russo A; Mitchell JB; Finkelstein E; DeGraff WG; Spiro IJ; Gamson J The effects of cellular glutathione elevation on the oxygen enhancement ratio. Radiat. Res. 103:232–239; 1985. [PubMed: 4023177]

[32]. Mallard WG; Ross AB; Helman WP NIST Standard Reference Database. Gaithersburg, MD: NIST; 1998 (version 3.0).

[33]. Griffith DM; Szocs B; Keogh T; Suponitsky KY; Farkas E; Buglyo P; Marmion CJ Suberoylanilide hydroxamic acid, a potent histone deacetylase inhibitor; its X-ray crystal structure and solid state and solution studies of its Zn(II), Ni(II), Cu(II) and Fe(III) complexes. J. Inorg. Biochem. 105:763–769; 2011. [PubMed: 21496451]

[34]. Harel S; Salan MA; Kanner J Iron release from metmyoglobin, methemoglobin and cytochrome-C by a system generating hydrogen-peroxide. Free Radic. Res. Commun. 5:11–19; 1988. [PubMed: 2853113]

[35]. Keefer LK; Nims RW; Davies KM; Wink DA "NONOates" (1-substituted diazen-1-ium-1,2-diolates) as nitric oxide donors: Convenient nitric oxide dosage forms. Methods Enzymol. 268:281–293; 1996. [PubMed: 8782594]

[36]. Camphausen K; Cerna D; Scott T; Sproull M; Burgan WE; Cerra MA; Fine H; Tofilon PJ Enhancement of in vitro and in vivo tumor cell radiosensitivity by valproic acid. Int. J. Cancer 114:380–386; 2005. [PubMed: 15578701]

[37]. Karagiannis TC; Harikrishnan KE; Assam E-O The epigenetic modifier, valproic acid, enhances radiation sensitivity. Epigenetics 1:131–137; 2006. [PubMed: 17965607]

[38]. Chen X; Wong P; Radany E; Wong JYC HDAC inhibitor, valproic acid, induces p53-dependent radiosensitization of colon cancer cells. Cancer Biother. Radiopharm. 24:689–699; 2009. [PubMed: 20025549]

[39]. Shoji M; Ninomiya I; Makino I; Kinoshita J; Nakamura K; Oyama K; Nakagawara H; Fujita H; Tajima H; Takamura H; Kitagawa H; Fushida S; Harada S; Fujimura T; Ohta T Valproic acid, a histone deacetylase inhibitor, enhances radiosensitivity in esophageal squamous cell carcinoma. Int. J. Oncol. 40:2140–2146; 2012. [PubMed: 22469995]

[40]. Samuni Y; Samuni U; Goldstein S The use of cyclic nitroxides as HNO scavengers. J. Inorg. Biochem. 118:155–161; 2013. [PubMed: 23122928]

[41]. Saelen MG; Ree AH; Kristian A; Fleten KG; Furre T; Hektoen HH; Flatmark K Radiosensitization by the histone deacetylase inhibitor vorinostat under hypoxia and with capecitabine in experimental colorectal carcinoma. Radiat. Oncol 7:165; 2012. [PubMed: 23017053]

[42]. Rogakou EP; Pilch DR; Orr AH; Ivanova VS; Bonner WM DNA double-stranded breaks induce histone H2AX phosphorylation on serine 139. J. Biol. Chem. 273:5858–5868; 1998. [PubMed: 9488723]

[43]. Stewart GD; Nanda J; Katz E; Bowman KJ; Christie JG; Brown DJG; McLaren DB; Riddick ACP; Ross JA; Jones GDD; Habib FK DNA strand breaks and hypoxia response inhibition

mediate the radiosensitisation effect of nitric oxide donors on prostate cancer under varying oxygen conditions. Biochem. Pharmacol. 81:203–210; 2011. [PubMed: 20888325]

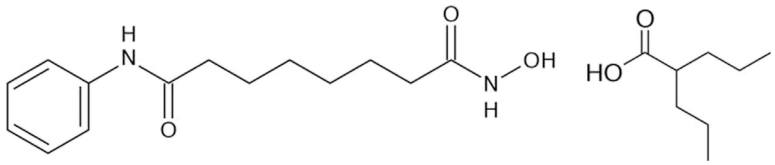

Fig. 1.
Structures of SAHA and valproic acid.

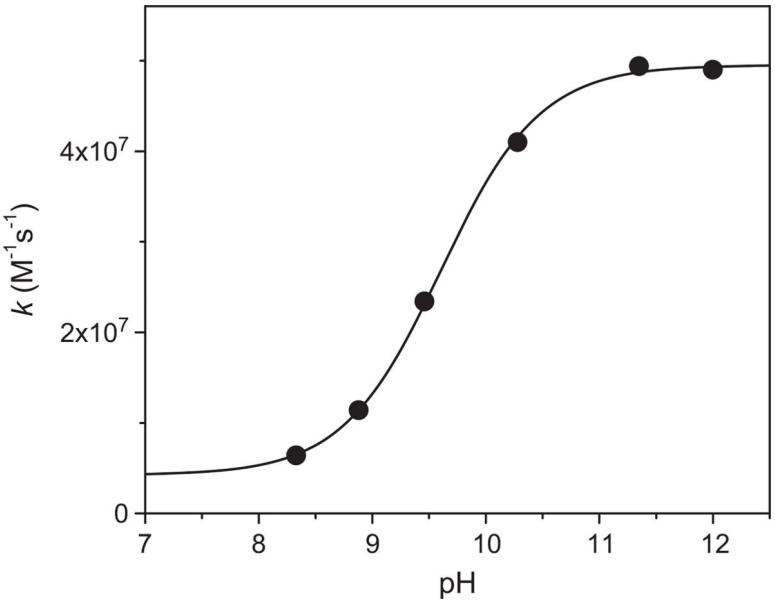

Fig. 2.

The pH dependence of the rate constant of $Br_2^{\bullet -}$ reaction with SAHA. The sigmoidal fit resulted in an upper value of $(4.9 \pm 0.1) \times 10^7$ M^{-1} s^{-1}, a lower value of $(3.0 \pm 0.7) \times 10^6$ M^{-1} s^{-1}, and $pK_a = 9.56 \pm 0.04$.

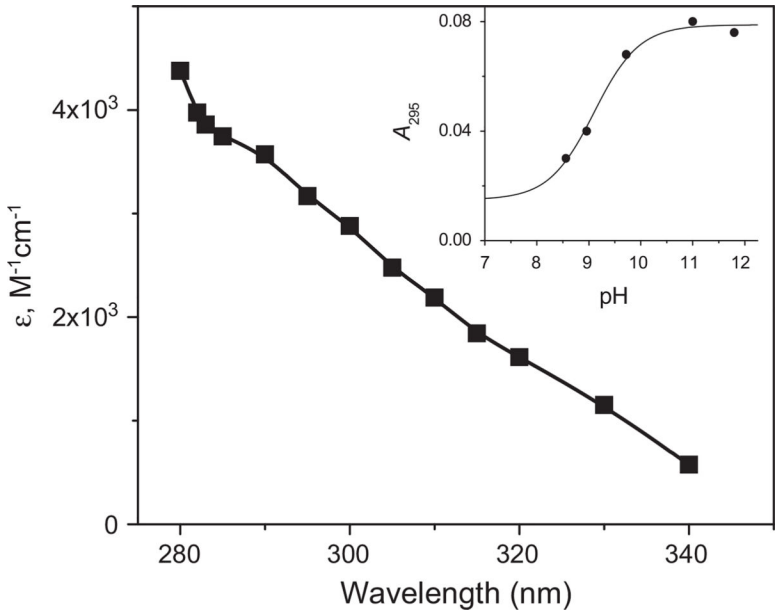

Fig. 3.

The absorption spectrum of $RC(O)NO^{\bullet-}$ was measured 20 μs after pulse irradiation of N_2O-saturated solution containing 0.2 mM SAHA and 0.2 M N_3^- at pH 11.4. (Inset) The dependence of the absorption at 295 nm on the pH measured at the end of the formation of the absorption reflecting a pK_a=9.1 ± 0.2. The dose was 4.8 Gy and the optical path 6.1 cm.

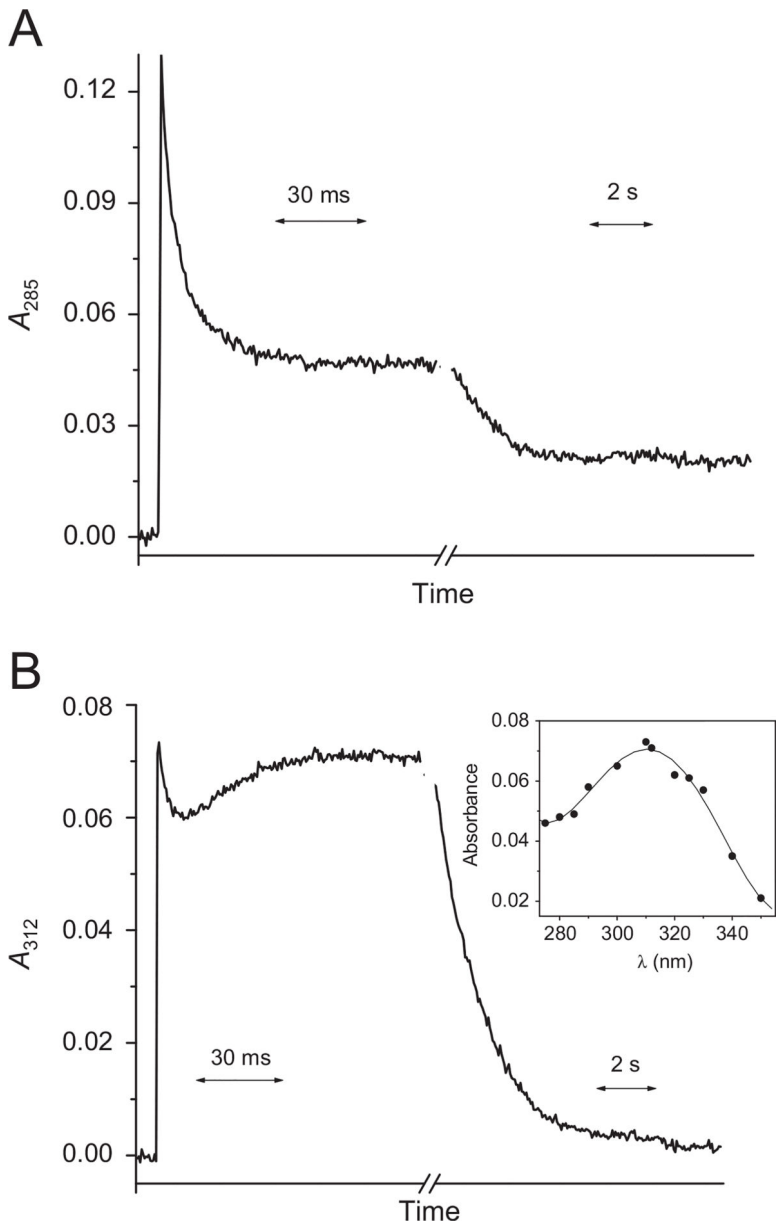

Fig. 4.

Kinetic traces obtained at (A) 285 nm and (B) 312 nm upon pulse irradiation (32 Gy/pulse) of N_2O-saturated solution containing 0.2 mM SAHA, 0.2 M NaN_3 at pH 11.4 (optical path 6.1 cm). (B, inset) The absorption of the transient species formed 100 ms after the pulse.

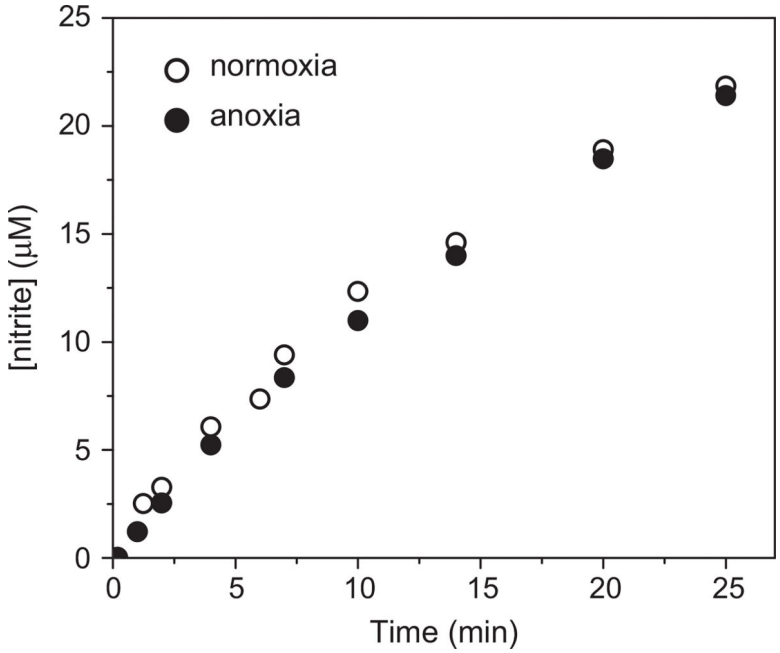

Fig. 5.

Accumulation of nitrite during the incubation of 1 mM SAHA with 5 μM $MbFe^{III}$ and 5 mM H_2O_2 in 10 mM phosphate buffer at pH 7.4 under aerobic (normoxia) or anoxic conditions.

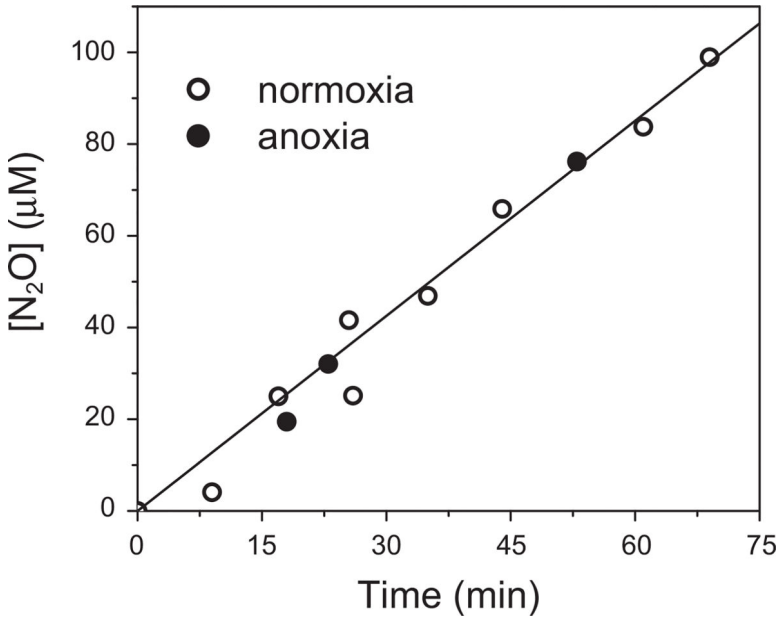

Fig. 6.

Accumulation of N_2O during the incubation of 2 mM SAHA with 30 μM $MbFe^{III}$ and 5 mM H_2O_2 in 10 mM phosphate buffer at pH 7.4 under aerobic (normoxia) or anoxic conditions.

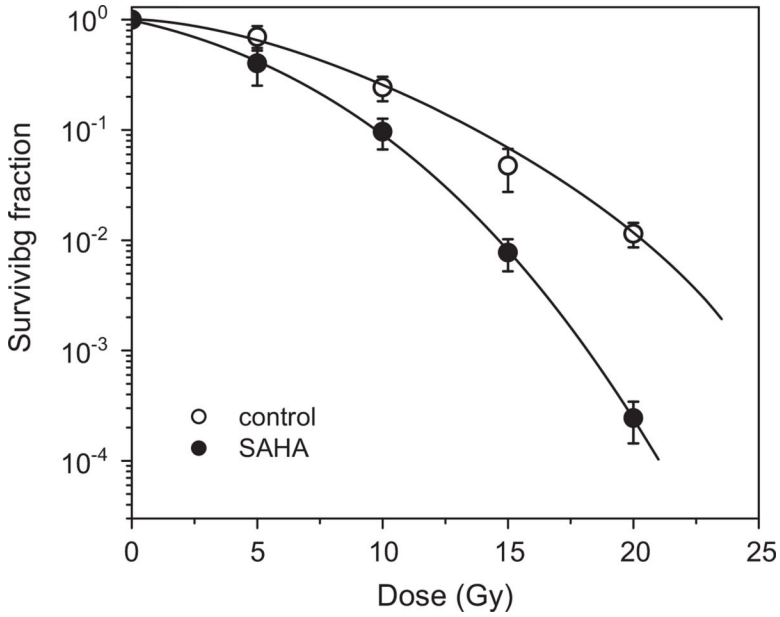

Fig. 7.

SAHA enhances the killing of irradiated hypoxic A549 cells. Cells were treated under aerobic conditions for 24 h with 2.5 μM SAHA, subjected to hypoxic conditions for 1 h, and then exposed to a range of radiation doses. The radiation survival curve was corrected for SAHA cytotoxicity. The mean $SER_{0.01}$ is 1.33 (n=2).

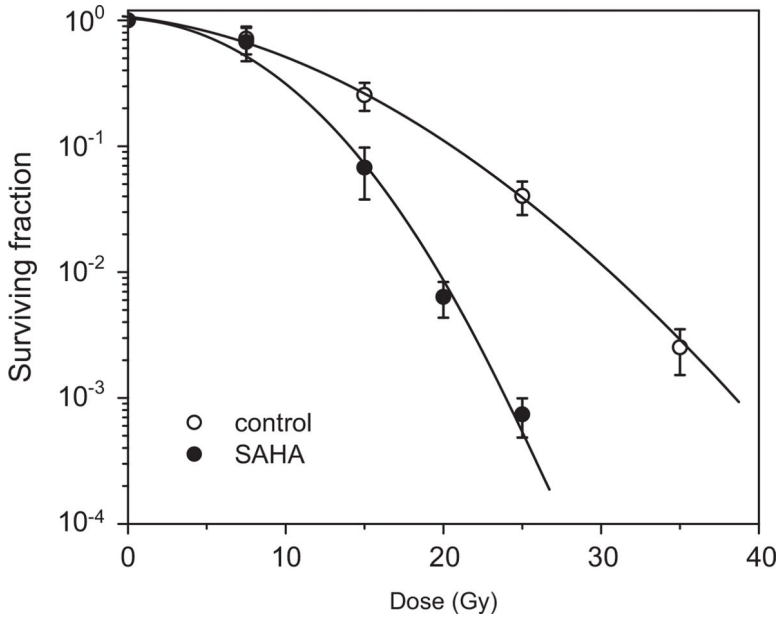

Fig. 8.

SAHA enhances the killing of irradiated hypoxic HT29 cells. The cells were treated under aerobic conditions for 24 h with 2.5 μM SAHA, subjected to hypoxic conditions for 1 h, and then exposed to a range of radiation doses. The radiation survival curve was corrected for SAHA cytotoxicity. The mean $SER_{0.01}$ is 1.59 (n=2).

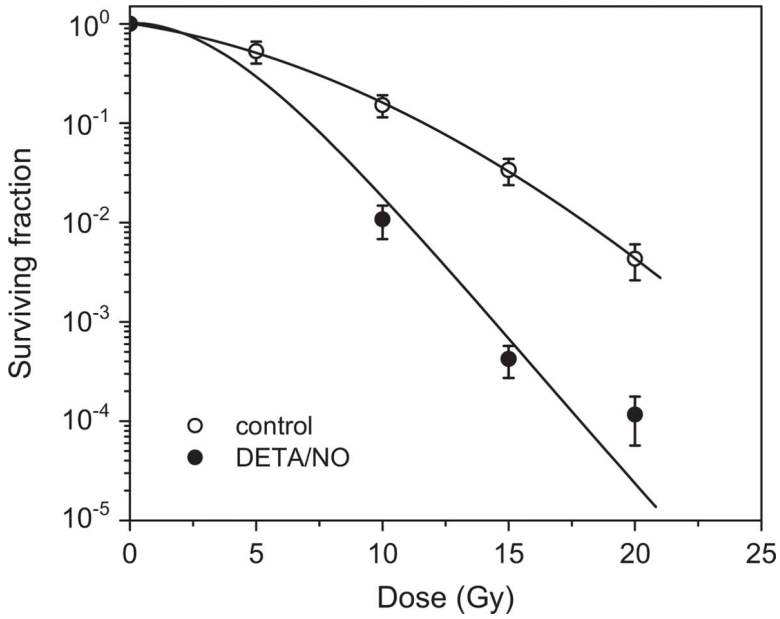

Fig. 9.

NO enhances the killing of irradiated hypoxic A549 cells. The cells were treated under aerobic conditions for 24 h with 1 mM DETA/NO, subjected to hypoxic conditions for 1 h, and then exposed to a range of radiation doses.

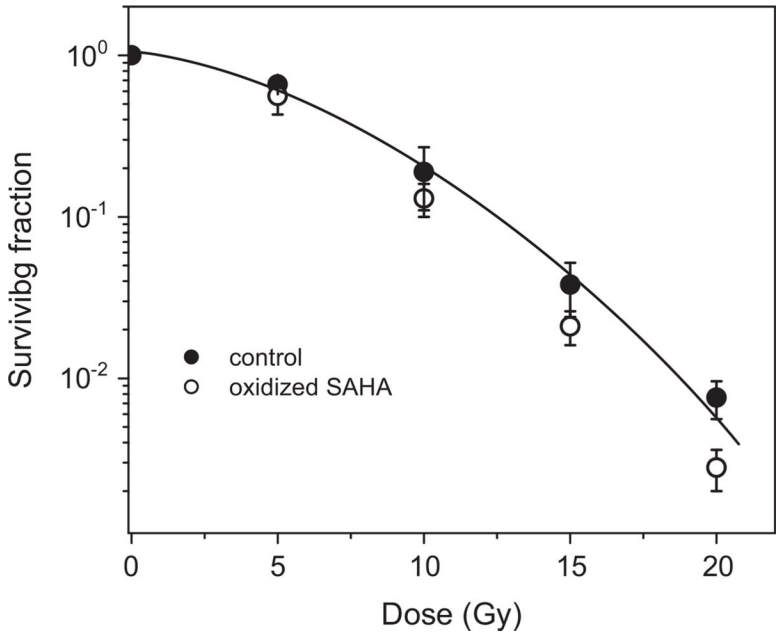

Fig. 10.

Effect of oxidized SAHA on the killing of irradiated hypoxic A549 cells. Cells were treated under aerobic conditions for 24 h with 2.5 μM oxidized SAHA, subjected to hypoxic conditions for 1 h, and then exposed to a range of radiation doses.

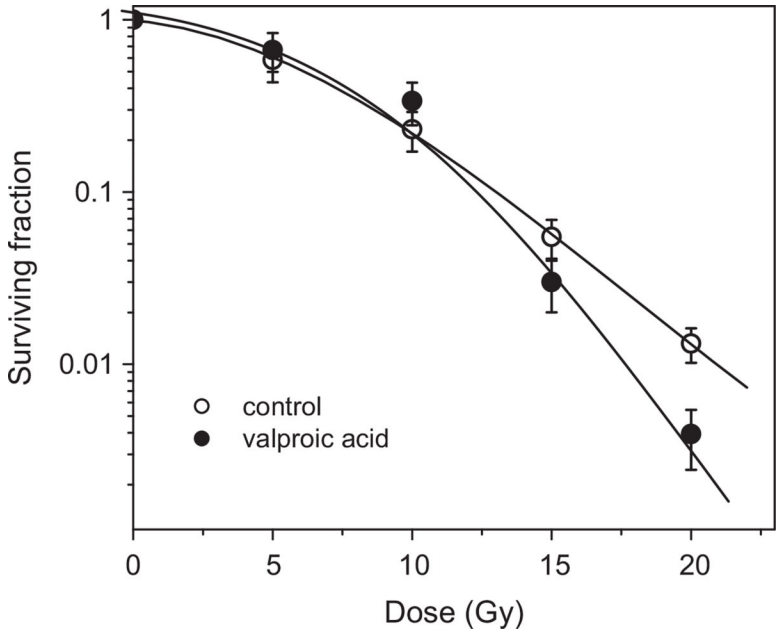

Fig. 11.

Effect of valproic acid on the killing of irradiated hypoxic A549 cells. The cells were treated under aerobic conditions for 24 h with 2 mM valproic acid, subjected to hypoxic conditions for 1 h, and then exposed to a range of radiation doses. The radiation survival curve was corrected for valproic acid cytotoxicity. The mean $SER_{0.01}$ is 1.17 (n=2).

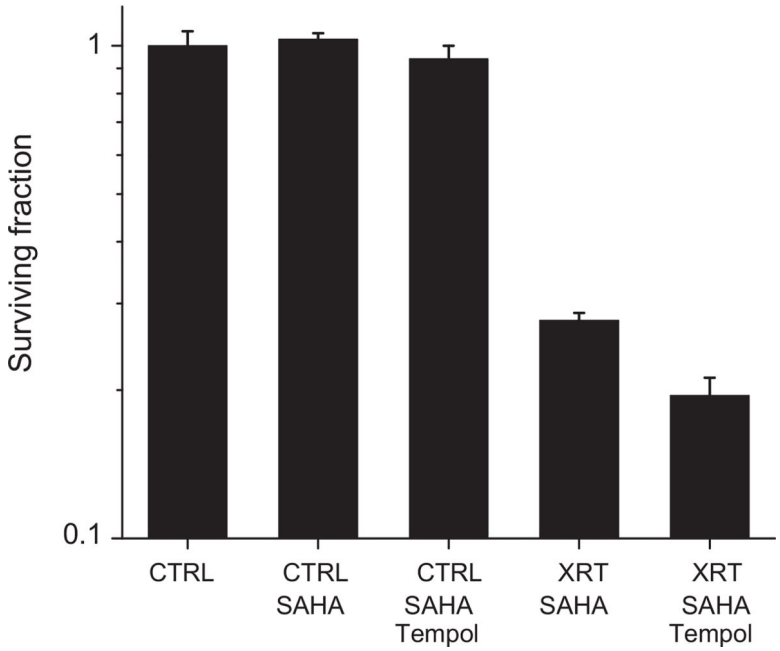

Fig. 12.

Effects of Tempol and SAHA on the killing of irradiated hypoxic HT29 cells. Cells were treated under anoxic conditions for 45 min with 2.5 μM SAHA and another 20 min with 1 mM Tempol and then exposed to 15 Gy radiation (XRT).

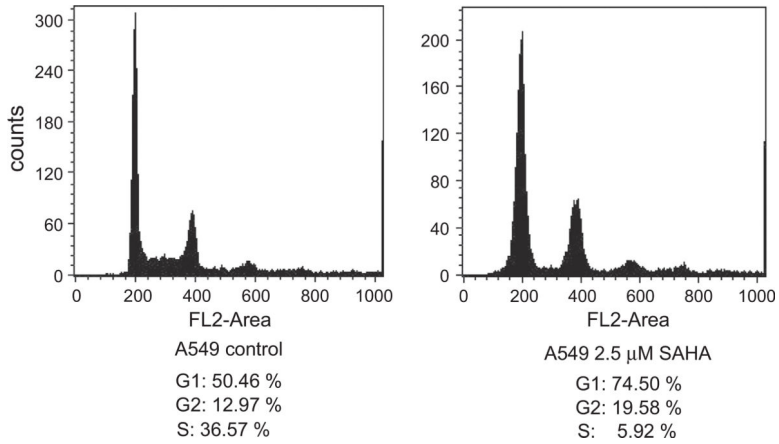

Fig. 13.

SAHA blocks A549 cells at the G1 stage of the cell cycle. The cells were treated for 24 h with 2.5 μM SAHA under aerobic conditions, subjected to hypoxic conditions for 1 h, and then analyzed using flow cytometry.

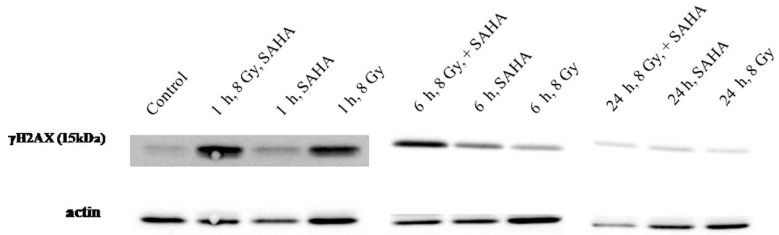

Fig. 14.

SAHA upregulates γ-H2AX levels 1 and 6 h after radiation. The A549 cells were treated for 24 h with 2.5 μM SAHA under aerobic conditions, subjected to hypoxic conditions for 1 h, and irradiated (8 Gy) and the levels of γ-H2AX were determined 1, 6, and 24 h after irradiation.

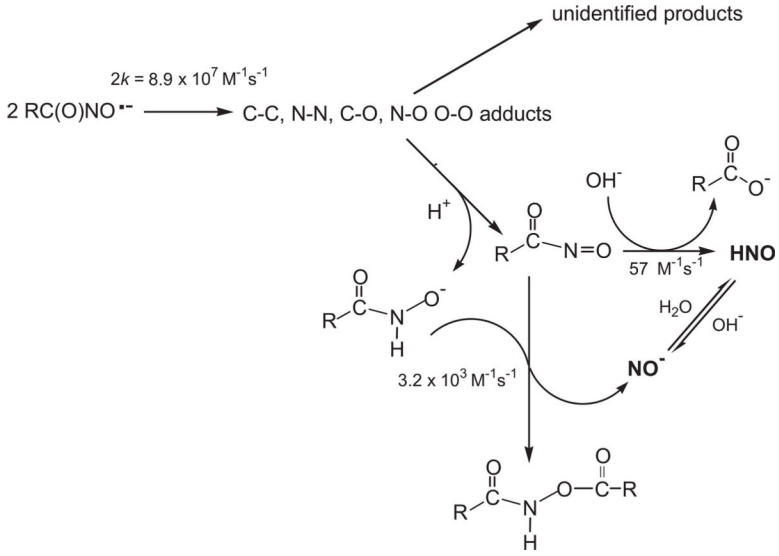

Scheme 1.

Proposed mechanism for the decomposition of $RC(O)NO^{\bullet -}$ derived from one-electron oxidation of SAHA in alkaline solutions.

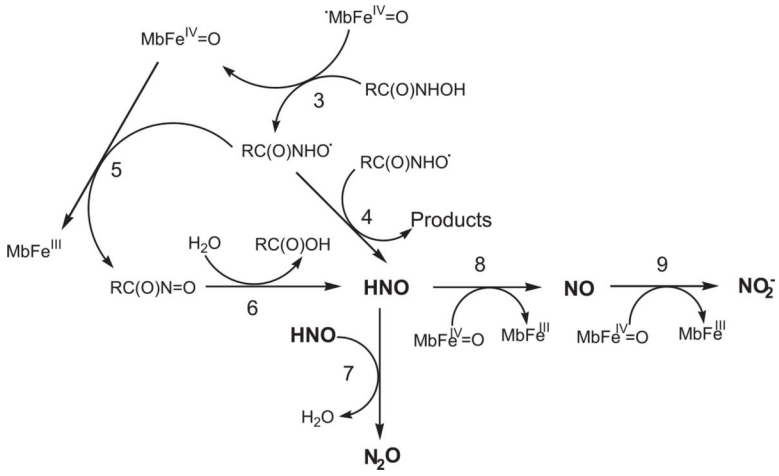

Scheme 2.

Proposed mechanism for the oxidation of RC(O)NHOH by the $MbFe^{III}/H_2O_2$ reaction system..